CHAPTER 7

CONVERGENCE PROPERTIES OF FOURIER MODE REPRESENTATIONS OF QUASIPATTERNS

Alastair M. Rucklidge

Department of Applied Mathematics, University of Leeds,
Leeds LS2 9JT, UK

Spatial Fourier transforms of quasipatterns observed in Faraday wave experiments suggest that the patterns are well represented by the sum of 8, 10 or 12 Fourier modes with wavevectors equally spaced around a circle. We show that nonlinear interactions of n such Fourier modes generate new modes with wavevectors that approach the original circle no faster than a constant times n^{-2}. These close approaches lead to small divisors in the standard perturbation theory used to compute properties of these patterns, and we show that the convergence of the standard method is questionable in spite of the bound on the small divisors.

1. Introduction

One well studied example of a pattern-forming instability is the Faraday wave problem of the formation of waves on the surface of a layer of fluid as it is driven by vertical vibrations. This system has been subjected to intensive scrutiny in laboratory experiments and has come to be regarded as an archetypal pattern forming system. Clear examples of pattern formation occur in a wide range of other systems, including Rayleigh–Bénard convection, liquid crystals in externally imposed electric fields, nonlinear optics, directional solidification, vibrated granular media, chemical reactions and catalytic oxidation.

The simplest patterns, stripes, squares and hexagons, have reflection, rotation and translation symmetries. A comprehensive and very successful theory has been developed to analyze the creation of these patterns from an initial featureless state. This theory, which is based on computing the amplitudes of the various waves (or modes) that make up the pattern, is known as equivariant bifurcation theory, and is expounded in detail in a series of texts (see, for example, [8]).

In order to apply rigorous mathematical theories to explain experimen-

tal results and other occurrences of pattern formation in the natural world, there are naturally a series of idealizations and approximations that must be made. One supposes that in the absence of any driving force, the system will remain featureless, and that if the forcing is turned up, it must reach a critical level before it can overcome any inherent dissipation in the system. If the level of forcing (which is a parameter under the control of the experimentalist) exceeds this critical value, the featureless state will be unstable, and any small disturbances will grow. These cannot grow for ever, and one possible outcome is that the system will settle down to a steady state with some degree of spatial structure: a pattern.

Two further idealizations are often made when computing the mathematical properties of patterns. First, the experimental boundaries are ignored, and so in effect the experiment is supposed to be taking place in a container of infinite size; and second, the observed pattern is supposed to have perfect spatial periodicity. By only considering patterns that are periodic in space, rigorous theory can be applied to prove the existence of stripe, square and hexagon (and other) solutions of the nonlinear partial differential equations (PDEs) that model the experimental situation. Given that in some highly controlled experiments the idealization of spatial periodicity appears to hold over dozens of repeats of the pattern, these assumptions are perfectly reasonable when the objective is to understand the nature of these periodic patterns.

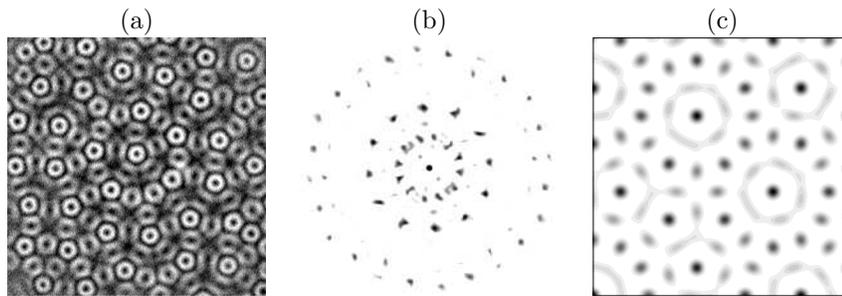(a)   (b)   (c)

Fig. 1.   Quasipatterns: (a) 12-fold quasipattern observed in a two-frequency forced Faraday wave experiment; (b) spatial Fourier transform, showing the 12-fold rotational order in spite of the absence of any translation symmetry (both from [1], with permission). (c) Synthetic quasipattern, constructed from the sum of 12 modes with wavevectors spaced equally around a circle; see equation (8).

However, experiments that are carried out in large domains are quite

A.M. Rucklidge

capable of producing patterns that cannot be analyzed in this way. A notable example of this is quasipatterns, which are most readily found in Faraday wave experiments in which a tray of liquid is subjected to vertical vibrations with two commensurate forcing frequencies[6]. A recent survey of experimental results can be found in [1], and one experimental example of a quasipattern is shown in figure 1a. This pattern is quasiperiodic in any horizontal direction, that is, the amplitude of the pattern (taken along any direction in the plane) can be regarded as a sum of modes with incommensurate spatial frequencies. In general, quasipatterns exhibit long range rotational order, most evident in their spatial Fourier transform (figure 1b), but they lack spatial periodicity. In this respect, there are obvious similarities with quasicrystals, which were discovered a decade earlier[11].

Models of quasipatterns have been developed by several researchers without the theoretical background required to justify their use (see below). These models are derived using a perturbation theory approach that is successful for periodic patterns; however, when the method is applied to the case of quasipatterns, a difficulty known as the problem of small divisors arises. This problem appears whenever quasiperiodic behavior is found in a nonlinear set of differential equations and attempts are made to use perturbation theory to compute the quasiperiodic solution by a series of approximations. In many cases, including the case of spatially periodic patterns, it can be proved that this process, if carried to the limit, will indeed converge to a true solution. However, in the case of quasiperiodic behavior, the corrections turn out not to be uniformly small, owing to the appearance of small numbers in the denominators, and convergence is called into question.

This difficulty was faced first by Poincaré in the context of celestial mechanics in the late 19th century. In the absence of any gravitational interaction between planets, each planet in the solar system orbits the Sun with its own period, and the system as a whole is quasiperiodic in time. Poincaré considered the question of whether or not the solar system is quasiperiodic given the presence of weak interactions between the planets. Formally, the problem could be solved by perturbation theory, but Poincaré realized that small divisors called convergence of the perturbation series into question.

The small divisor issue was resolved for this type of problem by Kolmogorov, Arnol'd and Moser (KAM) in the 1950's and 60's, who showed under what circumstances quasiperiodic behavior would be found (see, for
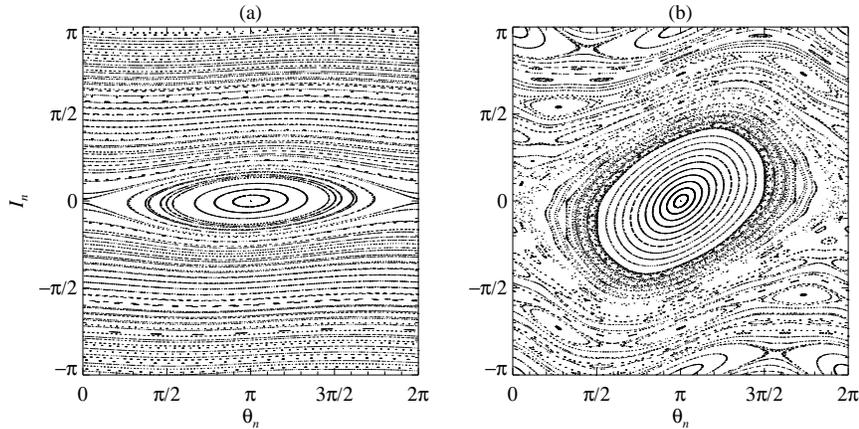
Convergence Properties of Fourier Mode Representations of Quasipatterns   127

Fig. 2.   Trajectories in the standard map (1): (a) $\varepsilon = 0.1$; (b) $\varepsilon = 0.8$. For small ε, several features are apparent: there are fixed points (at $(\theta, I) = (0, 0)$ and $(\pi, 0)$), periodic orbits and two types of quasiperiodic orbit: those that have a bounded range of θ (in an island centered on $(\pi, 0)$), and those for which θ increases or decreases monotonically. For larger ε, more islands are visible, as well as chaotic dynamics between the islands, and yet some quasiperiodic trajectories persist.

example, [15]). To take an example, consider the so-called standard map:

$$I_{n+1} = I_n + \varepsilon \sin(\theta_n), \qquad \theta_{n+1} = \theta_n + I_{n+1} \mod 2\pi, \qquad (1)$$

which models a freely rotating pendulum in the absence of gravity, subjected to periodic impulsive forces. When $\varepsilon = 0$, all trajectories are of the form $(\theta_n, I_n) = (\theta_0 + nI_0, I_0) \mod 2\pi$, and are periodic with period q if $I_0/2\pi = p/q$ is rational (with p and q integers), and quasiperiodic otherwise. Both periodic and quasiperiodic orbits lie on horizontal lines (invariant curves) in the (θ, I) plane, but the lines are made up of individual periodic points in the first case, while a quasiperiodic orbit will eventually visit a neighbourhood of each point on the line. When ε is perturbed away from zero (see figure 2a), the question is which of these families of trajectories will persist as invariant curves of the map? The essential content of the KAM theorem is that, for small enough perturbations, and for almost every irrational value of $I_0/2\pi$, there will be an invariant curve close to the unperturbed invariant curve, and the corresponding quasiperiodic trajectory survives the perturbation. The curves that persist are those that satisfy a Diophantine condition, that is, for which there are constants $K > 0$ and

$\delta > 0$ such that $I_0/2\pi$ satisfies

$$\left| p - \frac{I_0}{2\pi} q \right| \geq \frac{K}{(|p| + |q|)^\delta} \tag{2}$$

for every pair of integers p and q, apart from $(0,0)$. The exponent δ is an indication of the 'irrationality' of $I_0/2\pi$, so, for example, $(\sqrt{5} - 1)/2$ satisfies (2) with $\delta = 1$. In general, curves with smaller values of δ persist to larger values of the perturbation ε. Invariant curves with rational values of $I_0/2\pi$ are immediately broken up into elliptic and hyperbolic periodic points, with a web of chaotic trajectories near the hyperbolic equilibria (see figure 2b).

KAM theory has been applied successfully to a variety of problems in which small divisors arise, for instance quasiperiodicity in the solar system and in the dynamics of charged particles in tokamak magnetic fields. However, the methods of KAM (based around canonical coordinate transformations) were developed for problems in which quasiperiodicity occurs in only *one* direction (time), whereas quasipatterns are quasiperiodic in *two* spatial directions. For this reason, KAM theory is not applicable to quasipatterns, at least not directly, and either the theory must be extended to cover this case, or alternative methods must be developed. In principle, similar issues arise in solid-state quasicrystals, though the main theoretical approaches for these are developed around aperiodic Penrose tilings of the plane or three dimensional space, and around projecting higher dimensional periodic lattices down to three dimensions [10], whereas a wave-based approach is more natural for the fluid dynamical quasipatterns.

The purpose of this paper is to draw attention to some of the theoretical difficulties that are preventing progress in the development of a mathematical understanding of two-dimensional quasipatterns. We review progress that has recently been made in coming to terms with the small divisor problem [17]. Section 2 introduces a particularly simple pattern-forming PDE (the Swift–Hohenberg equation) and indicates how the small divisors arise. Limits on the magnitude of these small divisors are calculated in Section 3, and the perturbation theory for the quasipattern solution of the Swift–Hohenberg equation is concluded in Section 4, with an indication that the problem of small divisors does indeed cause the perturbation theory to fail. We conclude with general remarks in the last section.

2. Model Equations

One of the key mathematical questions concerning quasipatterns is one of *existence*: do PDEs that model pattern-forming problems have solutions that are quasiperiodic in space, along the lines of the experimentally observed pattern in figure 1a? Rather than try to answer this question in the context of a PDE that specifically models the Faraday wave problem, it seems sensible to start with the simplest possible pattern forming PDE: the Swift–Hohenberg equation [19]. In fact, considering the Swift–Hohenberg equation is not such a simplification, since many pattern-forming problems can be cast into this form, or variations [14]. The simplest variant is:

$$\frac{\partial U}{\partial t} = \mu U - (1 + \nabla^2)^2 U - U^3. \tag{3}$$

The equation is posed on the plane, with $\boldsymbol{x} = (x, y) \in \mathbb{R}^2$, and $U(x, y, t) \in \mathbb{R}$ supposed to be bounded as $(x, y) \to \infty$. The parameter μ represents the force that will drive the pattern formation.

In fact, stable quasipatterns are not observed in the Swift–Hohenberg equation with standard cubic nonlinearities, although they have been seen in numerical simulations with a modified linear term to allow marginally stable modes at two wavenumbers [12], in model equations that are essentially the Laplacian of the Swift–Hohenberg equation [3],[4], and in the Zhang–Viñals model of the Faraday wave experiment [20]. However, the issue here is one of existence of quasipatterns rather than their stability, so we focus on (3) as a model problem.

This PDE has a spatially uniform trivial solution $U(x, y, t) = 0$, and the stability of this solution can be investigated by linearizing (3). The linearized equation has wave-like solutions: $U = e^{st} e^{i\boldsymbol{k} \cdot \boldsymbol{x}}$, with growth rate s and wavevector $\boldsymbol{k}$, with the growth rate related to μ and $|\boldsymbol{k}|$ by $s = \mu - (1 - |\boldsymbol{k}|^2)^2$. This relation is plotted in figure 3a in the case $\mu = 0$: with this value of μ, all modes are damped (have negative growth rate) apart from those with wavenumber $|\boldsymbol{k}|$ equal to 1. With μ just above zero, modes with $|\boldsymbol{k}|$ close to 1 will grow, until the nonlinear term in (3) causes the amplitudes of these modes to saturate at a level related to the value of μ.

In many pattern forming problems, standard perturbation theory can be used to compute how the amplitude saturates, with the assumption that the parameter μ and the amplitude of the pattern are both very small. This degree of smallness is explicitly introduced as a small parameter $\varepsilon \ll 1$, and U is written in the form:

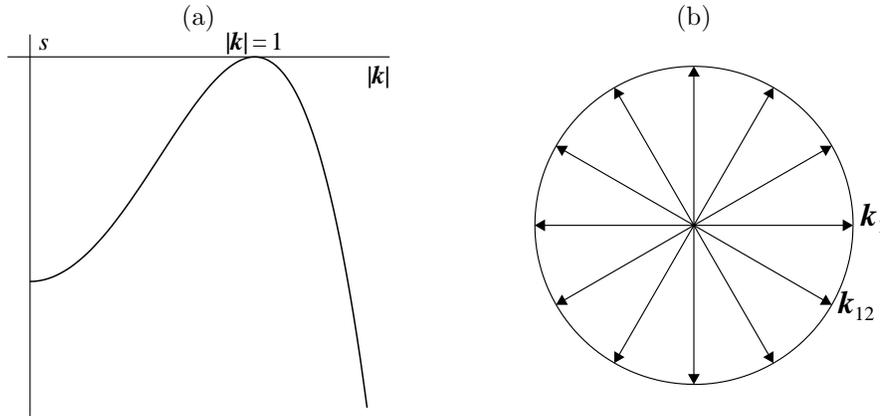$$U = \varepsilon U_1 + \varepsilon^3 U_3 + \varepsilon^5 U_5 + \dots \tag{4}$$

Fig. 3.   (a) Schematic growth (decay) rate s of a mode $e^{i\boldsymbol{k}\cdot\boldsymbol{x}}$, as a function of $|\boldsymbol{k}|$ at $\mu = 0$. Modes with $|\boldsymbol{k}| = 1$ are marginally stable. (b) 12 wavevectors on the circle $|\boldsymbol{k}| = 1$. Adding equal amounts of 12 modes with these wavevectors (numbered $\boldsymbol{k}_1$ to $\boldsymbol{k}_{12}$) results in the synthetic pattern in figure 1c.

The absence of even terms $(\varepsilon^2 U_2)$ is because of the symmetry $U \to -U$ in equation (3). The connection between the small forcing μ and the small parameter ε is made explicit by setting $\mu = \varepsilon^2$. The expansion (4) is inserted into the Swift–Hohenberg equation (3) and like powers of ε are collected together:

$$0 = \varepsilon\mathcal{L}(U_1) + \varepsilon^3 \left(U_1 + \mathcal{L}(U_3) - U_1^3 \right) + \varepsilon^5 \left(U_3 + \mathcal{L}(U_5) - 3U_1^2 U_3 \right) + \dots,$$

where, to make the presentation simpler, only steady patterns are considered. The linear differential operator $\mathcal{L}(U)$ is $-(1 + \nabla^2)^2 U$.

In order for this equation to be satisfied for all parameter values, the coefficient of each power of ε must separately be zero, and so the equation can be solved formally by considering each power of ε in turn. The leading order equation is

$$\mathcal{L}(U_1) = 0. \tag{5}$$

The operator $\mathcal{L}$ acting on a mode $e^{i\boldsymbol{k}\cdot\boldsymbol{x}}$ yields $-(1 - |\boldsymbol{k}|^2)^2 e^{i\boldsymbol{k}\cdot\boldsymbol{x}}$, which is zero only when $|\boldsymbol{k}| = 1$, so equation (5) has non-trivial solutions that are made up of linear combinations of modes with wavevectors $\boldsymbol{k}$ on the unit circle. Any set of such wavevectors is possible at this level, but a natural

choice to make when studying quasipatterns is

$$U_1(x, y) = \sum_{j=1}^{12} A_j e^{i\boldsymbol{k}_j \cdot \boldsymbol{x}},$$

where the 12 vectors $\boldsymbol{k}_1$ to $\boldsymbol{k}_{12}$ are equally spaced around the circle (figure 3b). This choice of modes is inspired by the evidence in the Fourier transforms of experimentally observed quasipatterns (as in figure 1b). In order for U to be real, the amplitudes must satisfy $A_{j+6} = \bar{A}_j$. Setting each A_j to the same real value results in a quasipattern of the form depicted in figure 1c.

At third order in ε, the equation to solve is:

$$\mathcal{L}(U_3) = -U_1 + U_1^3 = -\sum_{j=1}^{12} A_j e^{i\boldsymbol{k}_j \cdot \boldsymbol{x}} + \sum_{j=1}^{12} \sum_{k=1}^{12} \sum_{l=1}^{12} A_j A_k A_l e^{i(\boldsymbol{k}_j + \boldsymbol{k}_k + \boldsymbol{k}_l) \cdot \boldsymbol{x}}.$$
$$(6)$$

Notice that U_1^3 contains cubic interactions between the modes in U_1, which take the form of modes with all possible combinations of three of the 12 original wavevectors (allowing repeats). Some combinations (for example, $\boldsymbol{k}_1 + \boldsymbol{k}_1 + \boldsymbol{k}_7 = \boldsymbol{k}_1$) lie on the unit circle, but most ($\boldsymbol{k}_1 + \boldsymbol{k}_2 + \boldsymbol{k}_3$) do not. Modes with different wavevectors are orthogonal, so the coefficients of each mode on the left and the right of equation (6) must be equal. In particular, the coefficient of modes with wavevectors on the unit circle is zero on the left, since $\mathcal{L}$ acting on such a mode is zero. Setting the coefficient of (for example) $e^{i\boldsymbol{k}_1 \cdot \boldsymbol{x}}$ to zero on the right results in an equation relating the amplitudes of the modes:

$$0 = A_1 - 3(|A_1|^2 + 2|A_2|^2 + 2|A_3|^2 + 2|A_4|^2 + 2|A_5|^2 + 2|A_6|^2)A_1, \quad (7)$$

with similar equations resulting from the other modes. One solution of the amplitude equations is for all the amplitudes to be zero (the trivial solution); setting all amplitudes to have the same non-zero modulus results in a quasipattern. One particular solution is $A_1 = \ldots = A_{12} = 1/\sqrt{33}$, and so, in terms of the original variables, the pattern is:

$$U(x, y) = \sqrt{\frac{\mu}{33}} \sum_{j=1}^{12} e^{i\boldsymbol{k}_j \cdot \boldsymbol{x}} + \ldots \qquad (8)$$

This result suggests that the quasipattern solution is created when μ increases through zero, with an amplitude proportional to $\sqrt{\mu}$.

This might appear to be the end of the story: the amplitude of the quasipattern has been computed as a function of the driving force, and a

A.M. Rucklidge

little more effort leads to an estimate of the stability of the pattern. This kind of calculation has been carried out in a variety of situations, starting either from equations describing the Faraday wave experiment or other experiments, or just using considerations of the symmetry of the quasipattern [16],[7],[13],[2]. All these calculations result in amplitude equations similar to (7), and all suffer from two severe drawbacks.

The first drawback is that equation (7) determines only the amplitudes of the complex numbers A_j, and not their phase. In all, there are six free phases: two of these are fixed by considering resonances that occur at fifth order; two are genuinely free, and are associated with translating (but not changing) the pattern; and two phases (called phason modes) are not determined even by high-order resonances. In this context, the phason modes describe relative translations of two hexagonal sublattices generated by $\boldsymbol{k}_1$, $\boldsymbol{k}_3$, $\boldsymbol{k}_5$ and $\boldsymbol{k}_2$, $\boldsymbol{k}_4$, $\boldsymbol{k}_6$, and may play a role in long-wave instabilities of the quasipattern [5]. However, as they have a marked effect on the appearance of the pattern, they ought to be determined in a satisfactory theory without long-wave considerations.

The second drawback becomes apparent only when an attempt is made to compute higher order corrections to the pattern. Returning to equation (6), all modes with wavevectors on the unit circle have already been taken into account by solving (7). The remaining modes all have wavevectors off the unit circle ($|\boldsymbol{k}| \neq 1$), and so the linear operator $\mathcal{L}$ can be inverted to find U_3:

$$U_3 = - \sum_{|\boldsymbol{k}_j + \boldsymbol{k}_k + \boldsymbol{k}_l| \neq 1} \frac{A_j A_k A_l}{\left(1 - |\boldsymbol{k}_j + \boldsymbol{k}_k + \boldsymbol{k}_l|^2\right)^2} e^{i(\boldsymbol{k}_j + \boldsymbol{k}_k + \boldsymbol{k}_l) \cdot \boldsymbol{x}},$$

since the operator $\mathcal{L}^{-1}$ acting on a mode $e^{i\boldsymbol{k}\cdot\boldsymbol{x}}$ yields $-e^{i\boldsymbol{k}\cdot\boldsymbol{x}}/(1 - |\boldsymbol{k}|^2)^2$, defined as long as $|\boldsymbol{k}| \neq 1$.

However, if $|\boldsymbol{k}|$ is close to one, $\mathcal{L}^{-1}(e^{i\boldsymbol{k}\cdot\boldsymbol{x}})$ can be arbitrarily large. This does not pose difficulties for computing U_3, but continuing the calculation to higher order results in combinations of vectors that can come arbitrarily close to the unit circle. Specifically, U_3 involves sums of three of the original 12 vectors, and U_N will involve integer combinations of up to N of the 12 vectors $\boldsymbol{k}_1$ to $\boldsymbol{k}_{12}$. If the original choice of vectors had been two, four or six, in an attempt to describe striped, square or hexagonal patterns, the integer combinations of vectors arising at high order would not have come close to the unit circle, instead forming a lattice. Choosing 12 evenly spaced vectors leads to integer combinations of vectors that come arbitrarily close to the unit circle. Small divisors arise when the operator $\mathcal{L}$ is inverted, which raises

doubts as to whether or not the power series (4) for U will converge.

3. Small Divisors

Does the smallness of the small divisors arising from inverting $\mathcal{L}$ cause the sum (4) for $U(x,y,t)$ to diverge? To answer this question, the first stage is to derive a Diophantine-like condition for integer combinations of up to N of the 12 original vectors on the unit circle (such combinations arising at order N in the power series for U). It turns out that, for a given N, the smallest nonzero distance from the unit circle of a combination of N vectors is bounded above and below by a constant times N^{-2}.
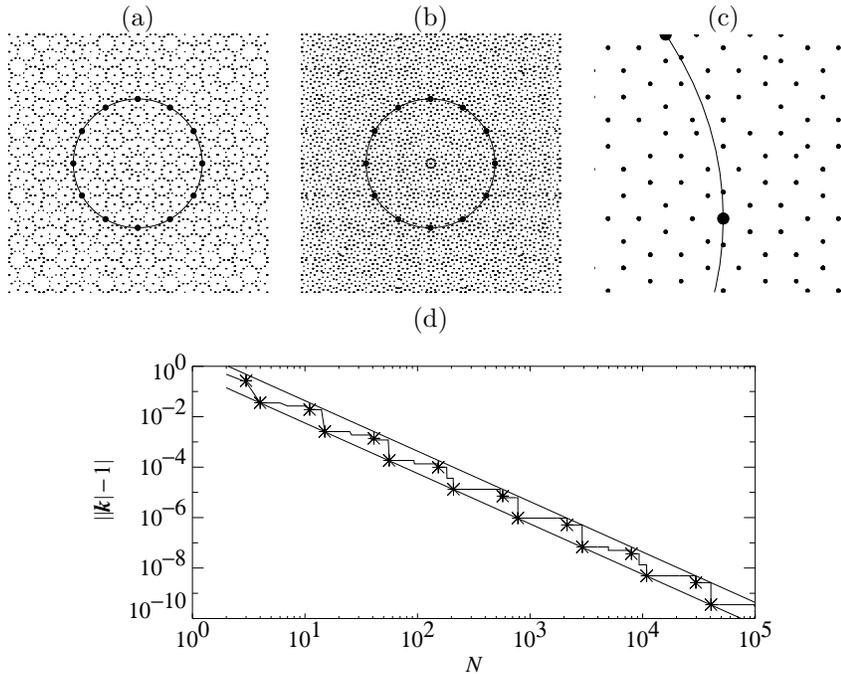

Fig. 4.   Positions of combinations of up to N of the original 12 vectors on the unit circle, with (a) $N = 11$, (b) $N = 15$; (c) detail of (b). The circle indicates the unit circle, $|\boldsymbol{k}| = 1$, the large dots are the original 12 wavevectors, and the small dots are integer combinations of these. Note how the density of points increases with N, and the proximity of points to the unit circle decreases with N. (d) Smallest nonzero distances from the unit circle $||\boldsymbol{k_m}| - 1|$ as a function of the total number of modes $|\boldsymbol{m}| = N$. Stars mark distances calculated from equation (10), and straight lines indicate the scaling N^{-2}. After [17].

An explanation of how this is derived begins with figure 4a–c, illustrating the locations of combinations of up to $N = 11$ and 15 wavevectors. Note how the density of points increases with N, and how the minimum distance between points and the unit circle goes down with N. Figure 4d shows results for the smallest nonzero distance from the unit circle as a function of the total number of vectors. The solid lines in figure 4d confirm numerically that the scaling for the distance to the unit circle is order N^{-2}, and the stars represent explicit combinations of wavevectors close to the unit circle, which were found as follows.

The vectors $\boldsymbol{k}_1$, $\boldsymbol{k}_2$, ..., $\boldsymbol{k}_{12}$ are labelled anticlockwise around the circle starting with $\boldsymbol{k}_1 = (1,0)$, with $\boldsymbol{k}_{j+6} = -\boldsymbol{k}_j$ (figure 3b). Integer combinations of N of these vectors can be written as $\boldsymbol{k_m} = \sum_{j=1}^{12} m_j \boldsymbol{k}_j$, with $|\boldsymbol{m}| = \sum_j |m_j| = N$. Including equal and opposite vectors $\boldsymbol{k}_j$ and $\boldsymbol{k}_{j+6}$ will only increase N without coming any closer to the unit circle, so only m_1, ..., m_6 are considered, but these are allowed to be negative. With this restriction, the squared length of a vector $\boldsymbol{k_m}$ is:

$$|\boldsymbol{k_m}|^2 = m_1^2 + m_2^2 + m_3^2 + m_4^2 + m_5^2 + m_6^2$$
$$+ m_1 m_3 + m_2 m_4 + m_3 m_5 + m_4 m_6 - m_5 m_1 - m_6 m_2$$
$$+ \sqrt{3}(m_1 m_2 + m_2 m_3 + m_3 m_4 + m_4 m_5 + m_5 m_6 - m_6 m_1).$$

This is of the form $|\boldsymbol{k_m}|^2 = 1 + p - rq$, where $r = \sqrt{3}$ is irrational and p and q are integers. If $p - rq$ is close to zero (that is, if r is well approximated by the rational p/q), then $|\boldsymbol{k_m}|^2$ can come close to 1 (but can only be exactly 1 if $p = q = 0$).

It is clear that the theory of continued fraction approximations of irrationals will be useful here. The continued fraction expression for $r = \sqrt{3}$ is:

$$r = \sqrt{3} = 1 + \cfrac{1}{1 + \cfrac{1}{2 + \cfrac{1}{1 + \cfrac{1}{2 + \cdots}}}}.$$

Since this irrational satisfies a quadratic equation with integer coefficients, $\sqrt{3}$ is called a quadratic irrational.

If the fraction is truncated after l terms, the successive fractions p_l/q_l that approximate $r = \sqrt{3}$ are given in table 7.9. The theory of continued

Table 7.9.   Continued fraction approximations to $r = \sqrt{3}$, as a function of the order l of the truncation.

	$l = 0$	1	2	3	4	5	6	7	8	9	10
$r = \sqrt{3}$	$\frac{p_l}{q_l} = \frac{1}{1}$	$\frac{2}{1}$	$\frac{5}{3}$	$\frac{7}{4}$	$\frac{19}{11}$	$\frac{26}{15}$	$\frac{71}{41}$	$\frac{97}{56}$	$\frac{265}{153}$	$\frac{362}{209}$	$\frac{989}{571}$

fractions for quadratic irrationals [9] shows that

$$\frac{K_1}{q_l^2} < \left| \frac{p_l}{q_l} - r \right| < \frac{K_2}{q_l^2} \qquad \text{and} \qquad \left| \frac{p_l}{q_l} - r \right| < \left| \frac{p}{q} - r \right|, \tag{9}$$

where K_1, K_2 are constants, q an integer satisfying $0 < q < q_l$. These inequalities mean that the truncated continued fraction expansions p_l/q_l approximate r well, but not too well, as l becomes large, and that if p_l/q_l is the truncation of the continued fraction approximation of an irrational r, no other fraction with a smaller denominator comes closer to r.

Apart from those vectors $\boldsymbol{k_m}$ that fall exactly on the unit circle (which would have $p = q = 0$), the relations in (9) can be used to show that $|\boldsymbol{k_m}|^2$ can approach 1 no faster than order N^{-2}:

$$\left| |\boldsymbol{k_m}|^2 - 1 \right| \geq \frac{K}{N^2},$$

where $|\boldsymbol{m}| = N$ and K is a constant – this lower limit is shown as a straight line in figure 4d. See Rucklidge & Rucklidge (2003) for more details.

The order N^{-2} rate of approach is indeed achieved by special combinations of vectors, which were found after a prolonged examination of the distances plotted in figure 4d. Choosing

$$\boldsymbol{k_m} = p_l \boldsymbol{k_4} + (q_l - 1)\boldsymbol{k_9} + (q_l + 1)\boldsymbol{k_{11}} = (1, p_l - \sqrt{3}q_l), \tag{10}$$

with $|\boldsymbol{m}| = N = p_l + 2q_l$ and $|\boldsymbol{k_m}|^2 - 1 = (p_l - \sqrt{3}q_l)^2$. As N (or equivalently, l or q_l) increases, p_l and q_l are related by $p_l \sim \sqrt{3}q_l + \mathcal{O}(1/q_l)$, so $q_l = \mathcal{O}(N)$, and $|\boldsymbol{k_m}|^2 - 1 = \mathcal{O}(N^{-2})$. These particular choices of $\boldsymbol{k_m}$ are plotted on the graphs in figure 4d as stars.

In summary, given an integer N, the vector $\boldsymbol{k_m}$ with $|\boldsymbol{m}| = N$ that comes closest to the unit circle (without being on the unit circle) satisfies

$$\frac{K}{N^2} \leq \left| |\boldsymbol{k_m}|^2 - 1 \right| \leq \frac{K'}{N^2},$$

for constants K and K', for 12 equally spaced original vectors. The numerical evidence in figure 4d suggests values $K = 0.56$ and $K' = 4.34$.

4. The Question of Convergence

The results of the previous two sections imply that when $\boldsymbol{k_m}$ is close to the unit circle, $\mathcal{L}^{-1}(e^{i\boldsymbol{k_m}\cdot\boldsymbol{x}})$ can be as large as a constant times $N^4 e^{i\boldsymbol{k_m}\cdot\boldsymbol{x}}$, with $N = |\boldsymbol{m}|$. This is so large that it clearly could lead to divergence of the power series (4) for U, particularly when nonlinear interactions of these large contributions are taken into account. This problem of small divisors is not just a feature of the particular Swift–Hohenberg equation (3) used for illustration here, but arises in any calculation of the properties of quasipatterns based on perturbation theory.
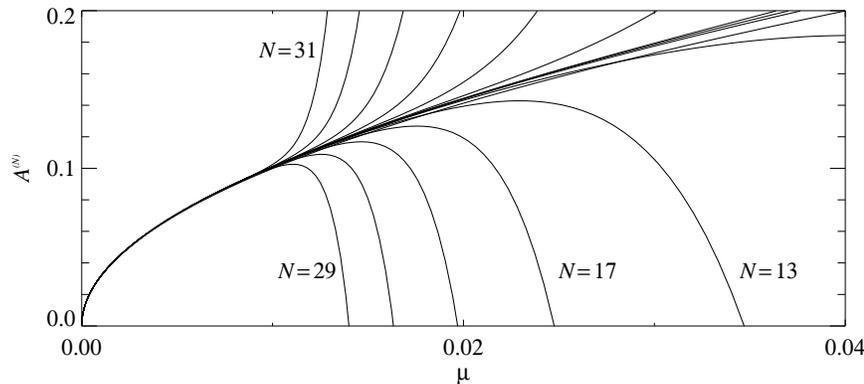

Fig. 5.   Amplitude $A^{(N)}$ as a function of μ, for different levels of truncation $N = 1, \ldots,$ 31. Increasing the order of truncation leads to graphs of $A^{(N)}$ that diverge for μ closer and closer to zero as N becomes larger. The amplitude has been scaled to remove a factor of $1/\sqrt{33}$. From [17].

This failure of convergence can be illustrated dramatically in the particular Swift–Hohenberg example by carrying out the perturbation theory calculation to high order (33rd order in this case). If the series (4) is truncated to include powers of ε up to and including $N + 2$, the resulting expression for $U^{(N)}$ is of the form

$$U^{(N)} = A^{(N)} \sum_{j=1}^{12} e^{i\boldsymbol{k}_j\cdot\boldsymbol{x}} + \text{other modes},$$

so $A^{(1)} = \sqrt{\mu/33}$, from (8). The amplitude $A^{(N)}$ of the basic quasipattern is shown as a function of μ in figure 5, for $N = 1, \ldots, 31$. In this calculation,

only modes with wavenumbers up to $\sqrt{5}$ were kept, to keep the total number of modes within manageable limits. Even so, there were more than 15000 modes generated at the highest order – without this truncation, there would have been almost 2 million. Since the modes that were dropped from the calculation were the most heavily damped, their contribution to the total amplitude was quite small (of the order of 1%), and restricting the number of modes in this way had no effect on how close combinations of wavevectors could get to the unit circle.

It is clear in figure 5 that, at each level of truncation N, the graph of $A^{(N)}$ against μ diverges at a value of μ that decreases as N becomes larger. The value of μ at which the sum up to order N diverges is related to the smallest distance from the unit circle achieved by combinations of N of the 12 original wavevectors. Since this distance goes to zero as N increases, the sum $A^{(N)}$ will continue to diverge closer and closer to $\mu = 0$. In contrast, the equivalent calculation for spatially periodic patterns has a non-zero radius of convergence [17].

5. Discussion and Speculation

The main conclusion of the calculation is that even if perturbation theory does generate a convergent series approximation to the quasipattern for small enough μ, the series certainly diverges if the parameter μ is bigger than about 0.01. It might be possible that the series does converge for smaller μ, though there is a strong argument that this is not the case. However, even if the series does diverge for all nonzero μ, a low-order truncation may still give a useful asymptotic approximation of the quasipattern, assuming that the equations do have a quasipattern solution. It is on this basis that other researchers have proceeded.

There are two related issues at stake. First, existence: do pattern forming PDEs (like the two-dimensional Swift–Hohenberg equation) have quasipattern solutions? A more general formulation of this question, using the Swift–Hohenberg equation as an example, becomes apparent by setting $\mu = \varepsilon^2$ in (3), scaling U by ε and seeking a steady solution. The resulting equation can be written as

$$\mathcal{L}(U) = \varepsilon^2(-U + U^3),$$

which incidentally demonstrates that this is not a singularly perturbed problem. When $\varepsilon = 0$, *any* linear combination of waves with wavevectors on the unit circle solves this equation. The question is, which of these solutions

A.M. Rucklidge

persist to small but positive ε? Current theory can so far only answer this question for those solutions that are spatially periodic. The limits on the rate of approach of wavevectors to the unit circle will play a central role in an eventual existence theory for quasipatterns.

The second issue is, given the small divisor problem, are there methods that yield useful approximations to quasipattern solutions? Standard perturbation theory does not converge sufficiently rapidly (or slowly) to provide an answer unequivocally one way or the other. However, if quasipattern solutions exist, then the series ought to provide an asymptotic approximation to those solutions. Nonetheless, this approach will be left with difficulties, such as the undetermined phason modes, and so should not be regarded as a reliable way of computing properties of quasipatterns.

What is needed is a method that converges more rapidly. Each order in the standard theory gains a factor of ε^2 as well as large factors from any small divisors that arise. There are other methods, developed for proofs of KAM theory, that converge more rapidly, and these may be required for a rigorous treatment of quasipatterns as well. The difference between the KAM situation and that of quasipatterns is that in the KAM case, the solutions of interest are quasiperiodic in only one dimension (time), while in the second, quasipatterns are quasiperiodic in two space directions.

There are alternative approaches to analysing quasipatterns, for instance based on successive approximation of a quasipattern by a periodic pattern with increasingly large periodicity, defined on square or hexagonal lattices. For example, approximate 12-fold quasipatterns can be constructed using modes with wavevectors $(1,0)$, $(2p_l q_l/(p_l^2 + q_l^2), (p_l^2 - q_l^2)/(p_l^2 + q_l^2))$ and so on, where $\frac{p_l}{q_l}$ is a truncated continued fraction approximation to $\sqrt{3}$. These generate patterns that are periodic on domains of size $p_l^2 + q_l^2$ times the original wavelength: 5, 34, 65, ..., for $l = 1, 2, 3, \ldots$, and have angles between their wavevectors of $36.9°$, $28.1°$, $30.5°$, ... The wavevectors all have unit wavenumber, since $(p_l^2 - q_l^2, 2p_l q_l, p_l^2 + q_l^2)$ form Pythagorean triplets – see Dawes, Matthews & Rucklidge (2003) for more details. Similarly, 12-dimensional representations of the group $D_6 \ltimes T^2$ can be chosen so that the modes are nearly equally spaced and yet they generate a hexagonal lattice ([18], and by allowing the wavevectors to have slightly different lengths, there are even more possibilities. The drawback with approximating quasipatterns by periodic patterns in these ways is that the range of validity of the normal forms derived shrinks to zero as the approximation improves.

Acknowledgments

References

[1]   Arbell, H. & Fineberg, J. 2002 . *Phys. Rev. E* **65**, 036224.
[2]   Chen, P. & J.Viñals 1999 . *Phys. Rev. E* **60**, 559–570.
[3]   Cox, S.M. & Matthews, P.C. 2001 . *Physica* **149D**, 210–229.
[4]   Dawes, J.H.P., Matthews, P.C. & Rucklidge, A,M. 2003 . *Nonlinearity* **16**, 615–645.
[5]   Echebarria, B. & Riecke, H. 2001 . *Physica* **158D**, 45–68.
[6]   Edwards, W.S. & Fauve, S. 1994 . *J. Fluid Mech.* **278**, 123–148.
[7]   Golovin, A.A., Nepomnyashchy, A.A. & Pismen, L.M. 1995 . *Physica* **81D**, 117–147.
[8]   Golubitsky, M. & Stewart, I. 2002 *The Symmetry Perspective: From Equilibrium to Chaos in Phase Space and Physical Space*. Basel: Birkhäuser.
[9]   Hardy, G.H. & Wright, E.M. 1960 *An Introduction to the Theory of Numbers, 4th edition*. Oxford: Clarendon Press.
[10] Janot, C. 1994 *Quasicrystals: a Primer, 2nd edition*. Oxford: Clarendon Press.
[11] Levine, D. & Steinhardt, P.J. 1984 . *Phys. Rev. Lett.* **53**, 2477–2480.
[12] Lifshitz, R. & Petrich, D.M. 1997 . *Phys. Rev. Lett.* **79**, 1261–1264.
[13] Lyngshansen, P. & Alstrom, P. 1997 . *J. Fluid Mech.* **351**, 301–344.
[14] Melbourne, I. 1999 . *Trans. Am. Math. Soc.* **351**, 1575–1603.
[15] Moser, J. 1973 *Stable and Random Motions in Dynamical Systems*. Princeton: Princeton University Press.
[16] Pismen, L.M. 1981 . *Phys. Rev. A* **23**, 334–344.
[17] Rucklidge, A.M. & Rucklidge, W.J. 2003 . *Physica* **178D**, 62–82.
[18] Silber, M., Topaz, C.M. & Skeldon, A.C. 2000 . *Physica* **143D**, 205–225.
[19] Swift, J. & Hohenberg, P.C. 1977 . *Phys. Rev. A* **15**, 319–328.
[20] Zhang, W. & J.Viñals 1996 . *Phys. Rev. E* **53**, R4283–R4286.

140   *A.M. Rucklidge*